Intricate coupling between ion–ion and ion–surface correlations in double layers as illustrated by charge inversion—combined effects of strong Coulomb correlations and excluded volume

2009 J. Phys.: Condens. Matter 21 424101

(http://iopscience.iop.org/0953-8984/21/42/424101)

J. Phys.: Condens. Matter **21** (2009) 424101 (16pp) doi:10.1088/0953-8984/21/42/424101

Intricate coupling between ion–ion and ion–surface correlations in double layers as illustrated by charge inversion—combined effects of strong Coulomb correlations and excluded volume

Roland Kjellander

Department of Chemistry, University of Gothenburg, SE-412 96 Gothenburg, Sweden

Received 28 March 2009
Published 29 September 2009
Online at stacks.iop.org/JPhysCM/21/424101

Abstract

Many-body correlations in electrolyte systems are important when the electrostatic coupling and/or the volume fraction of ions are not low. Such correlations are ignored in the traditional theories of electrolytes based on the Poisson–Boltzmann approximation. In the general case, the ion density profiles (ion–surface correlation functions) and the ion–ion correlation functions in diffuse electric double layers are strongly interdependent. Both have to be included in the treatment of the system to capture many essential properties. In this work the coupling between the ion–ion and ion–surface correlations and effects of this coupling are illustrated explicitly and graphically (visually). The average forces that act on the ions in the double layer are analysed. This leads to an understanding of mechanisms in action in the inhomogeneous electrolyte near a surface. Charge separation in an electrolyte outside an uncharged surface and charge inversion of highly charged surfaces are thereby used as examples of what insights can be gained by this kind of approach. Some links to mechanisms behind like-charge attraction are also discussed.

(Some figures in this article are in colour only in the electronic version)

1. Introduction

Many-body correlations have been the focus in modern theoretical treatments of electrolyte systems for a considerable time, but it is relatively recently that an understanding of the importance of such correlations has penetrated out to a wider section of the scientific community. The spreading of this understanding has perhaps been helped by some 'counterintuitive' and therefore intriguing findings in electrolyte theory applied to colloid chemistry and soft matter physics, like the phenomena of like-charge attraction and charge inversion (often called overcharging) caused by ion–ion correlations.

Charge inversion occurs when the number of counterions near a particle is larger than what is needed to neutralize its surface charge, so the particle behaves in many respects as if it has opposite charge compared to its bare charge. It is important to distinguish charge inversion caused by ion–ion correlations from that which occurs because of the chemical affinity of counterions to the surface, a quite common phenomenon [1]. In both cases the counterions are very strongly attracted towards the surface, which makes the concentration of counterions high there, but the mechanisms are different. In the correlation mechanism, the charge inversion is a consequence of the collective behaviour of the ions outside the surface and appears even in the absence of any specific interactions with the surface.

The like-charge electrostatic attractions make a radical break from the conventional picture of interactions between equally charged particles in electrolytes. This picture is based on the Derjauin–Landau–Verwey–Overbeek (DLVO) theory [2, 3] for interparticle interactions. It says that the

electrostatic double-layer interactions are always repulsive for equally charged particles, while attractions originate from van der Waals (vdW) forces between the particles. The fact that the vdW forces between the particles to a large extent are caused by correlations between electrons has been well known and accepted for a long time, but it has not been generally appreciated that the other charged particles in the system—the ions—also correlate and give rise to an attraction for essentially the same reason. While the presence of the latter kind of attraction was pointed out by Hill [4] in the 1960s (as correlations between charge fluctuations) and by Oosawa [5] in the 1970s, it was not until the 1980s that it was found that the ion–ion correlation effect was large enough to be important for aqueous electrolyte solutions of divalent ions [6, 7]. In such systems the double-layer pressure between two equally charged surfaces can be attractive for small surface separations, while it is always repulsive for large separations. The double-layer attraction can be much stronger than the vdW force. For monovalent aqueous electrolytes, on the other hand, the double-layer interactions are repulsive for all distances in most cases and the conventional picture then holds reasonably well.

There is, in fact, a common denominator between charge inversion and like-charge attractions. Both depend essentially on how strongly the counterions are attracted to the surface. To see this, let us linger for a while on the subject of like-charge attraction before we go on to the main theme of this paper, which is an analysis of the forces on the ions near a surface.

The great difference between monovalent and multivalent ions mentioned above is not caused by variations in the strength of the ion–ion correlation attraction. The correlation attraction between charged planar surfaces at short separations is, in fact, nearly the same for monovalent and multivalent ions. It is the strength of the *repulsive forces* between the surfaces that varies to a large extent for small separations, depending on the ion valencies [6]. As an example, let us consider two planar surfaces with a uniform surface charge density σ in contact with a bulk electrolyte solution. For simplicity we use the primitive model of electrolytes where the ions are charged hard spheres and the solvent is modelled as a dielectric continuum with relative permittivity (dielectric constant) equal to ϵ_r. The permittivity of vacuum is denoted ϵ_0.

One can quite easily show that the correlations between the ions in the slit between the two surfaces lead to an attractive electrostatic pressure contribution there that approaches the value $-\sigma^2/(2\epsilon_r\epsilon_0)$ when the surface separation becomes small (this comes from the electrostatic ion–ion correlation interactions across the midplane of the slit, see the appendix for a proof and other details). Note that this value is independent of the ionic valencies! Since some counterions must remain between the surfaces for small separations when $\sigma \neq 0$, their concentration increases when the surface separation decreases, which is the reason why the electric correlation attraction does not disappear for small separations. The increase in ion concentration makes, however, the repulsive contribution from the ideal pressure (momentum transfer across the midplane of the slit) to become very large for small surface separations, so the total double-layer pressure is always repulsive there when $\sigma \neq 0$. This repulsion, which is proportional to the ion density at the midplane, is stronger for monovalent counterions than for multivalent ones since a larger number of the former is needed to neutralize the surface charge (per unit area).

The important question is what happens when the separation increases. The attractive electrostatic correlation pressure remains initially at about the same magnitude, $-\sigma^2/(2\epsilon_r\epsilon_0)$, while the repulsive ideal pressure decreases rapidly since the ion concentration at the midplane goes down. If the repulsive pressure (including the repulsion from ion–ion collisions) goes down sufficiently, the attractive correlation pressure can dominate provided σ is large enough and then the total pressure between the surfaces becomes attractive (see, for example, [8] for the behaviour of the different contributions to the pressure). The attraction then appears in the multivalent case at large σ for two reasons: (i) the number of counterions is not so large and (ii) the counterions are attracted to the surfaces to a large extent, which makes the ion concentration around the midplane to be relatively low for the surface separations in question. Thus the appearance of double-layer attraction is closely linked to how strongly the counterions are attracted to the surfaces, i.e. how their concentration profile looks like. (Here we have considered the pressure between the surfaces. When the bulk electrolyte concentration is nonzero, the net double layer pressure is the difference between the pressure in the slit and in the bulk, but this does not change the conclusions provided σ is large enough.)

Thus, it is important to understand the mechanisms that govern the distribution of ions near a surface for both like-charge attractions and charge inversion caused by ion–ion correlations. More specifically it is a question of the coupling between ion–surface correlations (distributions of ions near a surface, i.e. concentration profiles) and ion–ion correlations (distributions of ions around an ion, i.e. pair distributions). Perhaps the most physical way to investigate the coupling between these correlations is to consider the average forces that act on the ions in the inhomogeneous electrolyte near the surface. The force on an ion originates from the ions and solvent in its surroundings, from the surface charge and the material behind the surface. In bulk the pair distributions of spherical ions are spherically symmetric and the average force on an ion is zero. Near a surface the pair distributions are distorted from spherical symmetry by the presence of the surface and the average force on an ion from the surrounding ions is therefore nonzero and can be calculated from the pair distributions. The average force f_i on an ion of species i is related to the potential of mean force w_i by the usual relationship between force and potential: $f_i = -\nabla w_i$. The potential of mean force and the ion density distribution n_i are related by the Boltzmann relation $n_i = n_i^{\text{bulk}} \exp(-\beta w_i)$, where n_i^{bulk} is the bulk density, $\beta = (k_B T)^{-1}$, k_B is Boltzmann's constant and T is the absolute temperature. This gives the link between the ion–surface and ion–ion correlations that we are going to pursue in this work. The important point is that various contributions to the force of different physical origin can be calculated which gives detailed information about the mechanisms in action. Thereby the fairly complicated interdependence of Coulomb correlations and excluded-volume effects can be explicitly illustrated and analysed.

Such an analysis of the structure of double layers based on forces has been done before for 1:1 and 2:2 electrolytes with ions of both equal and unequal sizes [9, 10]. Here we shall refine the analysis for the 2:2 case and extend it to 3:1 electrolytes. The main objective is thereby to illustrate the often intricate coupling between the ion–surface and ion–ion correlations in an explicit and graphical manner. This leads to a depth in understanding of these matters that is difficult to obtain by other means. The phenomena of charge separation in the electrolyte outside an uncharged surface and charge inversion at high σ are thereby used as examples of what insights can be gained by this kind of approach. Both phenomena have been observed in theoretical treatments of electric double layers for a very long time [11–15]. There have recently appeared many different approaches of various degrees of sophistication to treat charge inversion of particles; for recent reviews that cover many aspects of this topic see [16–18] and references therein. The importance of the influence of both Coulomb correlations and excluded-volume effects have been pointed out before, for recent examples see [19, 20]. In the current work we shall focus on what can be learned from an accurate theoretical treatment of ion–surface and ion–ion correlations in inhomogeneous electrolytes outside a charged surface in the primitive model. Thereby, we shall limit ourselves to conditions that are relevant for aqueous systems at room temperature and surface charge densities in the range that is of most interest in surface and colloid science.

2. Background

Let us consider a planar surface in contact with a bulk electrolyte solution of concentration c^{salt}. An ion of species i has a charge $q_i = Z_i e_0$, where Z_i is the valency and e_0 is the elementary unit charge. For simplicity we assume that all ions are charged hard spheres with the same diameter a. The surface has a uniform surface charge density σ. We will use a coordinate system with the z axis perpendicular to the surface and the x and y axes in the lateral directions. The origin is located at the distance of closest approach of the ionic centres to the surface. We will use the notation $\mathbf{r} = (x, y, z)$.

The ionic number density in the inhomogeneous electrolyte outside the surface is denoted $n_i(z)$ and the charge density equals

$$\rho(z) = \sum_i q_i n_i(z). \tag{1}$$

The mean electrostatic potential $\psi(z)$ satisfies Poisson's equation:

$$-\epsilon_r \epsilon_0 \frac{\mathrm{d}^2\psi(z)}{\mathrm{d}z^2} = \rho(z), \tag{2}$$

with the boundary condition $\psi(z) \to 0$ when $z \to \infty$.

In the PB approximation, where ion–ion correlations are ignored, the ion density profiles $n_i(z)$ outside a charged surface have monotonic decay towards the bulk density when z increases. The charge density $\rho(z)$ also decays monotonically. The number of counterions per unit area in a region outside the surface, $0 < z < z'$ for any z', is always less than required to neutralize both the surface charge density and the coions in the same region. Thus the sign of the total charge in $z < z'$ (including the surface charge) is always the same as that of σ while the sign of the charge in $z > z'$ is opposite. The mean electrostatic potential $\psi(z)$ has the same sign as σ and decays monotonically for all $z > 0$. For large z we have

$$\psi(z) \sim \frac{\sigma^0_{\text{PB}}}{\epsilon_r \epsilon_0 \kappa_D} \mathrm{e}^{-\kappa_D z} \qquad \text{(PB approximation)} \tag{3}$$

where σ^0_{PB} is (by definition) the effective charge density of the surface and κ_D is the inverse Debye length (defined from $\kappa_D^2 = \sum_i n_i q_i^2/(k_B T \epsilon_r \epsilon_0)$). The charge density decays like

$$\rho(z) \sim -\sigma^0_{\text{PB}} \kappa_D \mathrm{e}^{-\kappa_D z} \qquad \text{(PB approximation)} \tag{4}$$

when $z \to \infty$ (the decays in equations (3) and (4) are linked by Poisson's equation). The effective surface charge satisfies $\sigma^0_{\text{PB}} \sim \sigma$ when $\sigma \to 0$, but in general σ^0_{PB} is a nonlinear function of σ that tends to some constant when $\sigma \to \pm\infty$, i.e. σ^0_{PB} saturates for large surface charge densities. The value of this constant depends on the kind of electrolyte and its sign is the same as for σ (for symmetric electrolytes its absolute value is $(32\epsilon_r\epsilon_0 c^{\text{salt}} RT)^{1/2}$, where R is the gas constant).

None of these features of the PB theory are valid in the general case where ion–ion correlations are treated correctly. The PB approximation is generally valid only in the limit $\sigma \to 0$ *and* infinite dilution of electrolyte. For monovalent (1:1) electrolytes in aqueous solution at room temperature it holds, however, as a good approximation provided σ is not too large *and* the ionic bulk concentration is not too high. In other cases both quantitative and qualitative deviations occur. The deviations are particularly prominent at high electrostatic coupling, like for multivalent electrolytes where the Coulomb correlations are strong, but deviations occur also when the ion size is large.

In fact, one cannot strictly separate the effects of ionic charge and size. The anion–cation correlations give very important contributions to the properties of the electrolyte system. Because of the attraction between the ions the anion–cation contact distance strongly influences the magnitude of the effect of the electrostatics, in particular for highly charged ions. For cation–cation and anion–anion correlations the ionic size is less important because of the Coulombic repulsion. For highly charged ions, the ionic size must be quite large before the size matters in the latter cases (the size has to be larger than the 'Coulomb hole' created by the Coulombic repulsions). In the primitive model the ionic sizes we consider here are effective sizes that contain the effects of solvation. A small and/or highly charged ion will be strongly solvated and its effective size is therefore appreciably larger than its bare size.

A quantitative deviation from the PB prediction is that the decay length is not equal to the Debye length. The electrostatic potential $\psi(z)$ decays for large z like in equation (3) when the concentration is not too high, but with a decay parameter κ that is different from κ_D and with a different prefactor of the exponential function [21–23]. The decay parameter satisfies $\kappa^2 = \sum_i n_i q_i q_i^0/(k_B T \epsilon_r \epsilon_0)$, where q_i^0 is the effective charge of the ions of species i in bulk solution (cf the definition of κ_D above). For multivalent ions q_i^0 differs substantially from q_i except at high dilution and hence κ can be very different

from κ_D. This is an effect of the strong ion–ion correlations. The fact that the prefactor in the decay of $\psi(z)$ differs from the PB prediction means that the effective charge density σ^0 of the surface (as defined from the prefactor in analogy to equation (3)) is different. This too is an effect of the ion–ion correlations. For large surface charge densities σ^0 does not saturate in the way predicted by the PB theory and it does not need to have the same sign as σ (i.e. charge inversion may occur) [23, 24]. Furthermore, for asymmetric electrolytes σ^0 is not proportional to σ when $\sigma \to 0$ and it is nonzero when $\sigma = 0$. These facts will be further explored in this work.

In general, the functional form of the decay of the potential $\psi(z)$ and the charge density profile $\rho(z)$ for large z is determined by the bulk solution; the decay length is the same as for the ion–ion pair distributions in the bulk phase (more specifically, the charge distribution around an ion in the bulk phase and the charge density profile outside the surface decay in general with the same κ) [21, 22, 25]. A further consequence of this fact is that, when the bulk electrolyte concentration is increased, the profile and the potential turn oscillatory at the same concentration as the pair distributions in the bulk does. We then have for large z

$$\rho(z) \sim \text{const} \times \cos(\omega z + \vartheta)\, \mathrm{e}^{-Kz},$$

where ω and K are determined by the bulk solution. The parameter ϑ is a phase factor that depends on the surface properties, which the prefactor 'const' also does. Thus, an oscillatory profile is not due to some property of the surface and it will, for example, be oscillatory irrespective of the value of σ. Only the amplitude and the phase of the oscillations are surface-dependent. The charge distribution outside the surface will consist of an infinite series of 'layers' with alternating positive and negative net charges, although the magnitude diminishes exponentially fast. This behaviour is the common one in molten salts, but occurs also in electrolyte solutions when the electrolyte concentration is high enough.

When the bulk electrolyte concentration is lower than the threshold for the oscillatory correlations, there can, however, be one or a couple of oscillations in the immediate vicinity of the surface when σ is sufficiently large. After these oscillations the profile decays for larger z in a monotonic exponential manner. In such cases there is a layer just outside the surface with a net charge of opposite sign to that of σ followed by a layer with the same sign as σ. The number of counterions near the surface then exceeds the amount needed to neutralize the surface charge. This effect of ion–ion correlations has been known for a long time [11, 13–15] and constitutes the phenomenon of charge inversion we mentioned in section 1. Contrary to the oscillatory profiles for large z just discussed, this is a true surface-induced phenomenon (the two phenomena can, however, occur simultaneously). The excess counterions are not sitting *at* the surface, they are located as a diffuse layer *near* the surface. This excess of counterions makes the electrostatic potential far from the surface to have a sign opposite to that of σ, i.e. the effective charge σ^0 has an inverted sign. Thus it appears from a distance as if the surface has inverted its sign of charge.

Note that layering of ions outside a surface can also occur because of crowding of counterions near the surface when σ is high [11, 26]. Then two or more layers of counterions can form next to the surface without the occurrence of charge inversion. Here we shall only treat the case where charge inversion occurs and this as a consequence of strong ion–ion correlations.

3. Density profiles and pair distributions of inhomogeneous electrolytes

The ion density profiles outside charged surfaces can be accurately calculated by integral equation theory at the pair distribution level in the inhomogeneous electrolyte solution (see the appendix for details). In these kinds of theories both the anisotropic pair distributions and the density profiles are self-consistently calculated. Thereby one achieves much higher accuracy than simpler integral equation theories, like those that utilize isotropic pair correlation functions from bulk to calculate density profiles of the inhomogeneous fluid (see the appendix). Furthermore, the pair distributions can be used to analyse various mechanisms acting in the system, which we are going to do here.

In the current work the anisotropic reference hypernetted chain (ARHNC) [27] and the anisotropic hypernetted chain (AHNC) [28] approximations are used. The former gives pair distributions and density profiles in excellent agreement with simulations (often within the accuracy of the simulation) [27, 29]. The AHNC approximation, which is somewhat simpler numerically, gives equally good results [7, 8, 29, 30] except when the local ionic density is very high, which, for example, can happen for monovalent counterions near a highly charged surface. For multivalent counterions these kinds of ion densities are reached for very high surface charge densities (higher than those relevant here). Furthermore, the approximation does not work for multivalent ions at very low electrolyte concentrations and very high electrostatic coupling [31, 32], but such conditions are, however, not of relevance in this work. Thus, the use of these approximations gives a very good account of the properties of the systems we shall discuss.

The typical situation where charge inversion occurs due to ion–ion correlations is depicted in figure 1. It shows the charge density profile $\rho(z)$ for an electric double layer outside a surface with $\sigma = -0.160$ C m^{-2} (1.0 nm^2 per unit charge ($-e_0$)) in contact with a 0.35 M aqueous 2:2 electrolyte solution as calculated in the ARHNC approximation [9]. The ionic diameter is $a = 0.425$ nm and the temperature is $T = 298$ K. The charged surface is located to the left of $z = 0$ and the bulk electrolyte lies to the right outside the figure. The figure also shows the ion–wall distribution function $h_i(z)$, which describes the relative deviation of the ion density from the bulk value and is defined from

$$h_i(z) = g_i(z) - 1 = \frac{n_i(z) - n_i^{\text{bulk}}}{n_i^{\text{bulk}}}, \tag{5}$$

where $g_i(z) = n_i(z)/n_i^{\text{bulk}}$. The charge density $\rho(z)$ is proportional to the difference between $h_+(z)$ and $h_-(z)$:

$$\rho(z) = q_+ n_+ [h_+(z) - h_-(z)]$$

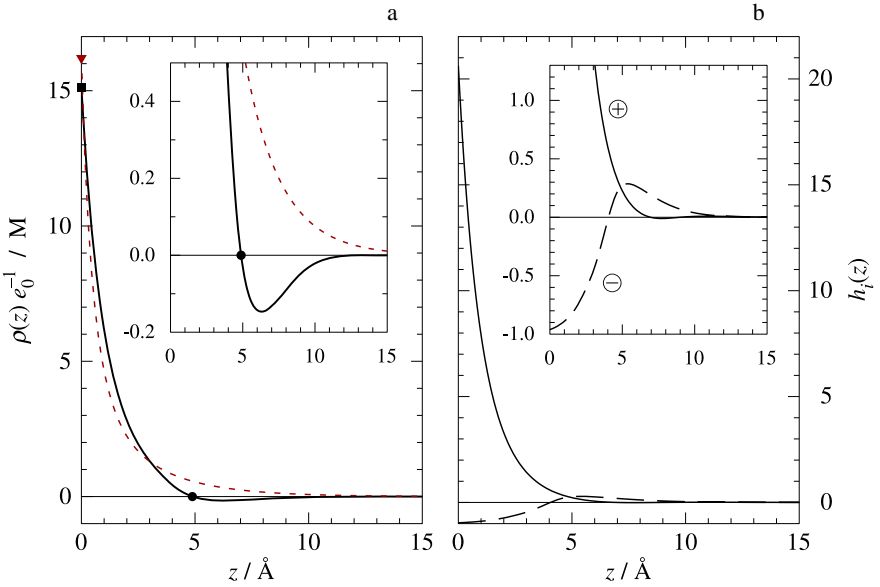

Figure 1. (a) Charge density profile $\rho(z)$ and (b) ion–wall distribution function $h_i(z)$ for a diffuse electric double layer outside a wall with surface charge density $\sigma = -0.160\ \mathrm{C\,m^{-2}}$ (1.0 $\mathrm{nm^2}$ per unit charge ($-e_0$)) in contact with a 0.35 M aqueous 2:2 electrolyte solution. In (a) the full line shows the profile calculated with proper consideration of ion–ion correlations, while the dashed line shows the Poisson–Boltzmann (PB) prediction that neglects such correlations. The filled circle indicates the point where the charge density changes sign. The filled square shows the contact density at the wall surface and the filled triangle shows the corresponding PB prediction. In (b) the full line is the distribution function $h_+(z)$ for counterions (cations) and the dashed line is $h_-(z)$ for the coions (anions). The insets show the same plots on an expanded ordinate scale.

and changes sign at $z \approx 5$ Å (marked with a black circle in the left panels of the figure), which is where $h_+(z)$ and $h_-(z)$ cross.

The total charge (per unit area) to the right of the circle, $z > 5$ Å, is negative (same sign as the surface charge). Electroneutrality then demands that the total charge in $z < 5$ is positive (i.e. the sum of charges of the surface and the diffuse layer in $0 < z < 5$). Thus, the number of counterions per unit area in the region, $0 < z < 5$, is larger than that required to neutralize both the surface charge density and the coions in the same region, i.e. charge inversion (overcharging) has occurred.

The PB prediction for $\rho(z)$ is also shown in the figure and here the total charge in $z < z'$ for any z' is always negative while the charge in $z > z'$ is positive as mentioned earlier in section 2. In the interval 0 Å $< z \lesssim 3$ Å the actual charge density (from ARHNC) is larger than the PB prediction except in a tiny interval at contact with the surface, where the PB charge density is higher. Both these features are relevant as we are going to see; the latter is due to a lower contact density of counterions at the surface compared to the PB prediction. The charge inversion disappears when σ approaches zero (not shown), so the qualitative behaviour is then more similar to the PB prediction, but quantitatively there are still differences, see, for example, reference [11, 23].

The charge inversion is associated with the diffuse 'layer' of mainly counterions near the surface; for the case in figure 1 it has a width of about 5 Å. Half of the counterions in this layer are located within 1 Å from the surface and 75% within 2 Å. Virtually no coions are located at $z \lesssim 2$ Å. The surface charge is neutralized by the charge located in $z < 3.5$ Å. The charge in 3.5 Å $< z < 5$ Å corresponds to an excess equal to 3% of the surface charge (in absolute value). This charge is a measure of the charge inversion and it is neutralized by the excess coions in $z > 5$ Å.

Figure 2 shows the corresponding charge density profiles for the case of a 0.1 M aqueous 3:1 electrolyte solution ($c^{\mathrm{salt}} =$ 95 mM) for a range of surface charge densities from $\sigma = -0.267$ to $-0.0032\ \mathrm{C\,m^{-2}}$ (corresponding to 0.6–50 $\mathrm{nm^2}$ per unit charge) and an uncharged surface, $\sigma = 0$. In this case the AHNC approximation has been used in the calculations. The trivalent ions are counterions to the surface, $a = 0.45$ nm and $T = 298$ K. For high values of σ (low area per unit charge), the charge density profiles are very similar to figure 1, while for low σ the curves change character. In the latter cases both anions and cations are depleted near the surface, the trivalent cations to a larger extent on a relative scale than the monovalent anions. The ion–wall distribution functions $h_i(z)$ for the uncharged case, $\sigma = 0$, are shown together with $\rho(z)$ in figure 3, where we see the large depletion of trivalent ions near the surface. The resulting negative charge density near the surface leads to a build up of trivalent ion concentration some distance away from the surface, so $\rho(z)$ behaves from the maximum onwards similar to the cases with charged surfaces.

The point where the charge density changes sign from positive to negative (marked by a circle for each curve in the right panes of figure 2) moves to higher z values when σ decreases in all cases shown. Like in the 2:2 case above, the number of counterions in the region between the surface and the circle is larger than that required to neutralize both the surface charge density and the coions in the same region, so charge inversion has occurred. This is true for all cases *including* the uncharged surface, so the latter behaves when

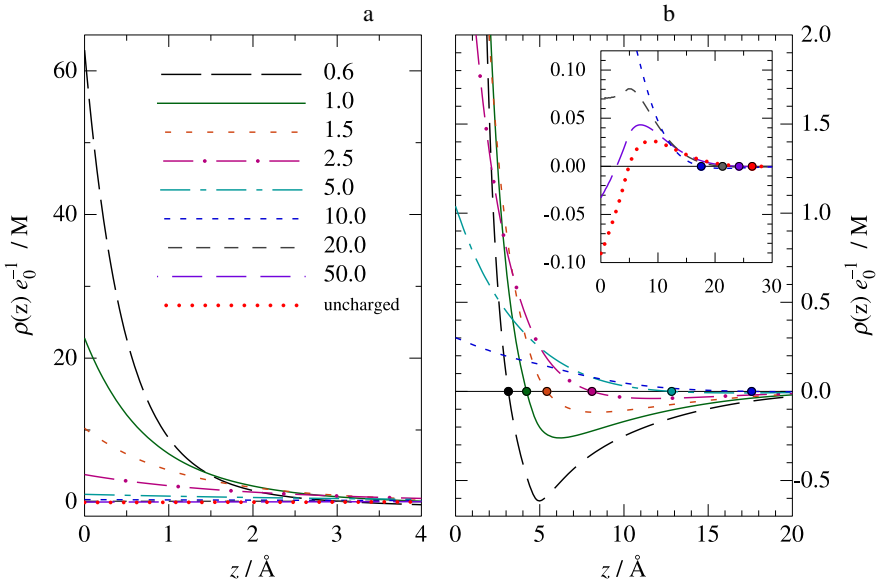

Figure 2. (a) Charge density profiles for 0.1 M 3:1 aqueous electrolyte solution near a surface with different surface charge densities ranging from $\sigma = -0.267$ to -0.0032 C m^{-2} (corresponding to 0.6–50 nm^2 per unit charge as shown in the caption inside the panel) and an uncharged surface, $\sigma = 0$. The trivalent ions are counterions to the surface. (b) The same curves on a different scale for the cases 0.6–10 nm^2 per unit charge. The inset shows the curves for the cases 10–50 nm^2 per unit charge and the uncharged surface on a further expanded ordinate scale. The filled circles indicate the points where the charge density changes sign from positive to negative values with increasing z in the respective cases.

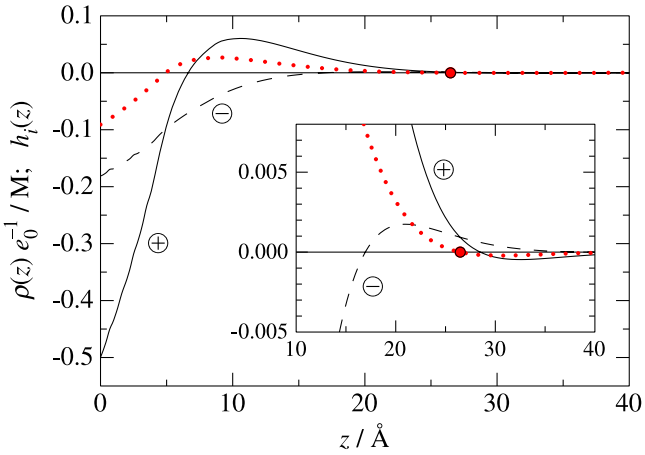

Figure 3. Charge density profile (dotted curve) and ion–wall distribution functions (marked ⊕ for trivalent cations and ⊖ for monovalent anions) for 0.1 M 3:1 electrolyte solution near an uncharged surface. The charge density profile is the same as the dotted curve in figure 2. The inset shows the same curves for large z on an expanded ordinate scale.

seen from a large distance as if the surface is weakly positively charged despite that $\sigma = 0$. For the case 1.0 nm^2 per unit charge ($\sigma = -0.160$ C m^{-2}, same σ as for the 2:2 case above) the sign change of $\rho(z)$ occurs at $z = 4.2$ Å (the circle in the figure) and the surface charge is neutralized by the diffuse layer charge in $z < 1.8$ Å. The charge in 1.8 Å $< z <$ 4.2 Å corresponds to an excess equal to 12% of the surface charge (in absolute value). This charge is neutralized by the excess coions to the right of the circle in the figure, $z >$ 4.2 Å. The corresponding numbers for 0.6 nm^2 per unit charge ($\sigma = -0.267$ C m^{-2}) are the sign change at $z = 3.1$ Å, neutralization in $z < 1.1$ Å and excess of 15% on either side of the circle (positive to the left and negative to the right). For 2.5 nm^2 per unit charge ($\sigma = -0.064$ C m^{-2}) the numbers are $z = 8.1$ Å, $z < 4.7$ Å and 6%.

For the uncharged surface the sign of $\rho(z)$ changes twice; at $z = 4.9$ and 26 Å, where the latter corresponds to the sign change for the charged surfaces we have discussed so far and the former exists only for very weakly charged surfaces. The total charge in $z < 4.9$ Å is -2.3×10^{-3} C m^{-2} (70 nm^2 per unit charge). This charge is neutralized by an excess of cations in 4.9 Å $< z <$ 23 Å, i.e. total charge from anions and cations are equal in $z <$ 23 Å. The excess of cations continues up to the sign change of $\rho(z)$ at $z = 26$ Å (the circle in the figure), but the total excess charge to the left of the circle is only 10^{-5} C m^{-2} and an equal amount of opposite sign to the right of the circle.

The important feature is the separation of charge that happens close to the surface despite that $\sigma = 0$ and it has consequences for particles that enter into this region. Nevertheless, the separation of charge around the circle in the figure and the residual charge density for large z is of some interest in principle despite that the effect is very small here. In the inset of figure 3 this behaviour is seen as the slightly negative charge density for large z (to the right of the circle), where the charge density contribution from the anions dominates over that from the cations. Thus charge inversion has taken place and the effective surface charge density σ^0 *is positive for all* $\sigma \leqslant 0$ for the 3:1 electrolyte investigated (remember that σ^0 by definition has the same sign as $\psi(z)$ for large z and hence the opposite sign to $\rho(z)$ there). This is different from 2:1 electrolytes (with divalent cations) [24]

where the effective surface charge has the *same* sign as the bare surface charge for small negative σ, but eventually turns positive due to charge inversion when σ becomes more negative (note that in [24] the anions are divalent and the cations monovalent, but here we have inverted all charges). For both 3:1 and 2:1 electrolytes an uncharged surface has a nonzero effective charge, but it is accordingly positive for 3:1 and negative for 2:1. For the 2:2 case, on the other hand, the effective charge for $\sigma = 0$ must be exactly zero due to symmetry (provided the anions and cations only differ by the sign of their charges).

Let us now return to nonzero σ. In all cases the charge inversion happens in a diffuse layer that is several ångströms wide. Thus it is not appropriate to think about this phenomena as an adsorption of counterions *at* the surface, i.e. as a layer of ions in direct contact with the surface. Some of the properties of the system may be modelled as a layer of ions at the surface, but this kind of approach misses the three-dimensional liquid features of the system. If the ions have a specific affinity to the surface, i.e. they are brought there, for instance, by some specific short-ranged nonelectrostatic interaction, the situation can, however, be quite different. Then a layer of ions can be appropriate. In this work we restrict ourselves to charge inversions associated solely with strong ion–ion correlations, i.e. when such specific interactions are absent. In correlation-driven inversions the diffuse layer characteristics of the inhomogeneous electrolyte near the surface are important in most cases of practical interest.

4. The environment of each ion in the double layer

What, precisely, is causing the charge inversion? For this to happen, the counterions near the surface must on average experience a sufficiently strong force directed towards the surface and/or the coions experience a force directed in the opposite direction, forces that are stronger than those predicted by the PB theory which does not show any charge inversion. Let us consider an arbitrary ion of species i near a surface. We denote this ion as 'ion I'. The average force that acts on ion I is due to interactions with the surface and with the ions around the ion. In the PB theory the latter interactions are calculated under the assumption that ion I does not affect the distribution of the other ions around it and that there are only electrostatic forces. The force is thereby calculated from the unperturbed charge density distribution $\rho(z)$ despite that the neighbourhood of ion I must have a charge density that is perturbed by the interactions with the ion. This simplification is a consequence of that the ion–ion correlations are neglected. The interaction energy (potential of mean force) that ion I experiences is thereby equal to $q_i\psi(z)$ in the PB theory, where ψ is given by equation (2), i.e. the standard PB relationships.

Let us now consider the actual situation for ion I and its environment. No other ion can come closer to ion I than a distance a between the ion centres. There must therefore be a cavity of radius a around the ion where no other ionic charge can enter. This is depicted in figure 4(b) which shows a contour plot of the unperturbed charge density distribution $\rho(z)$, but where we have cut a hole with radius a around ion I (here assumed to be a cation located 3 Å from the surface). The contour plot outside the cavity shows the same density distribution as in panel a of the figure, which is the same as in figure 1(a).

The charge density outside the cavity is, however, not unperturbed by the interactions with ion I as assumed in figure 4(b). It is polarized by the electrostatic interactions with ion I and the density around the ion is also affected by the hard core interactions (excluded-volume effects in the presence of the cavity). The resulting charge density distribution around ion I is depicted in figure 4(c). We see that the positive charge of ion I repels other positive ions (counterions to the surface), which makes the charge density above and below the ion in the figure to be smaller than in the unperturbed case in panel (b). Furthermore, the attraction of negative ions (and repulsion of positive ones) causes a build up of a negative charge density to the right of the ion in the figure. The actual electrostatic force that ion I experiences is due to this perturbed charge density around it. In the PB approximation one neglects both the cavity and the polarization. Instead one assumes that the charge density is $\rho(z)$ everywhere, even inside ion I.

Before we continue, let us make it very clear what figure 4(c) really shows. There are two equivalent ways to describe it. In the first, we pick an arbitrary ion in the electrolyte (ion I) and follow it in time (in the example we have picked a cation). We now look at its environment from the perspective of the ion. Each time ion I is located 3 Å from the surface we record the positions of all other ions in the system. We do this for a long time and obtain a large number of records of particle positions. In all these records particle I is located 3 Å from the surface and the other ions are in various locations in the available space. The average charge distribution from these records is what is depicted in the figure. Incidentally, if we instead would calculate the average cation and anion distributions from the records, we would obtain the cation–cation and cation–anion pair distributions for the case when a cation (ion I) is 3 Å from the surface. (Note that if we keep *all* records of the particle positions, i.e. not only those where ion I is 3 Å from the surface, the average charge density from *all* these records becomes equal to $\rho(z)$ and the anion and cation distributions become equal to the ion density profiles.) The second way to describe figure 4(c) is that it shows the average charge distribution around ion I when it is held fixed at a point 3 Å from the surface and all other ions are free to move. That the two different ways are equivalent follows from the fact that the translational and configurational degrees of freedom are independent of each other in classical statistical mechanics, so it does not matter whether ion I is mobile or stationary.

The charge distribution shown in figure 4(c) is calculated from the pair distributions obtained in the ARHNC approximation, where all ions of each species are treated in exactly the same manner. The corresponding charge distribution around an anion and around a cation at various distances from the surface is shown in figure 5, i.e. for various choices of 'ion I' and positions of it. Note that all ions around ion I are fully interacting and correlating with each other, so if we look at the

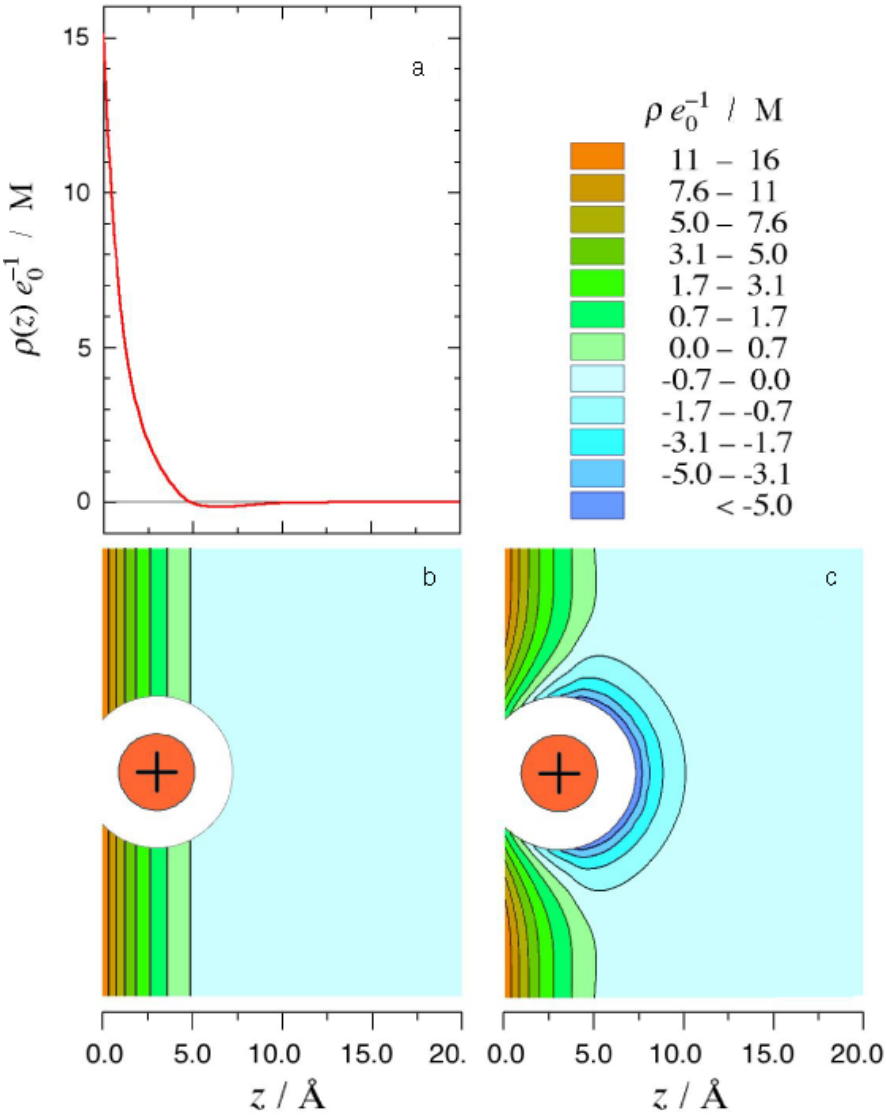

Figure 4. Charge density in a 2:2 electrolyte near a charged wall for the same system as in figure 1. (a) The charge density profile $\rho(z)$, i.e. the same as the full curve in figure 1(a). (b) The same $\rho(z)$ shown as a contour plot in a cross-section perpendicular to the surface, but with a cavity cut out around a counterion (cation $\oplus$) located 3 Å from the surface. The cavity shows the region where no ionic centres can enter because of hard core exclusion and its radius is equal to the ionic diameter. The wall surface is located to the left of the figure and $z = 0$ indicates the point of closest approach of the ion centres to the wall. The bulk electrolyte lies to the right of the figure. (c) The actual average charge distribution $\rho^{(2)}$ around the cation when ion–ion correlations are properly considered. The difference between the charge distributions in (c) and (b) is the 'polarization effect' in the surrounding electrolyte due to the interactions with the ion. Comment for greyscale printouts of the figure: the charge density is positive close to the wall and negative beyond $z \approx 5$ Å in panels (a) and (b). In panel (c) the charge density to the right of the cation is negative.

environment of each and every one of them from the perspective of the ion we would obtain the same average distributions as those in figure 5. In panels (a)–(d) of figure 5 we see how the charge density profile near the surface is distorted when a counterion (cation) is brought towards the surface. The other counterions between the ion and the surface are repelled away from the ion. At the same time the ion atmosphere around the ion, which is spherically symmetric when the ion is far from the surface, also becomes distorted. Similarly, for a coion (anion) we see the corresponding distortions in panels (e)–(h), but here the counterions are strongly attracted towards the region between the ion and the surface. They are attracted by both the anion and the negative surface charge.

5. Forces acting on the ions

Let us now consider the forces that act on ion I for various distances z from the surface. Due to cylindrical symmetry around an ion near a planar surface, the only nonzero component of the average force lies in the direction perpendicular to the surface. A force is counted positive when it is directed outwards from the wall (in the positive z direction) and negative when it is directed towards the wall. The electrostatic force, $f_i^{\mathrm{el}}(z)$, on the ion equals the Coulomb force from the charge distribution depicted in figure 5 and from the surface charge density. The force from the charge distribution varies in a complicated fashion with z since the

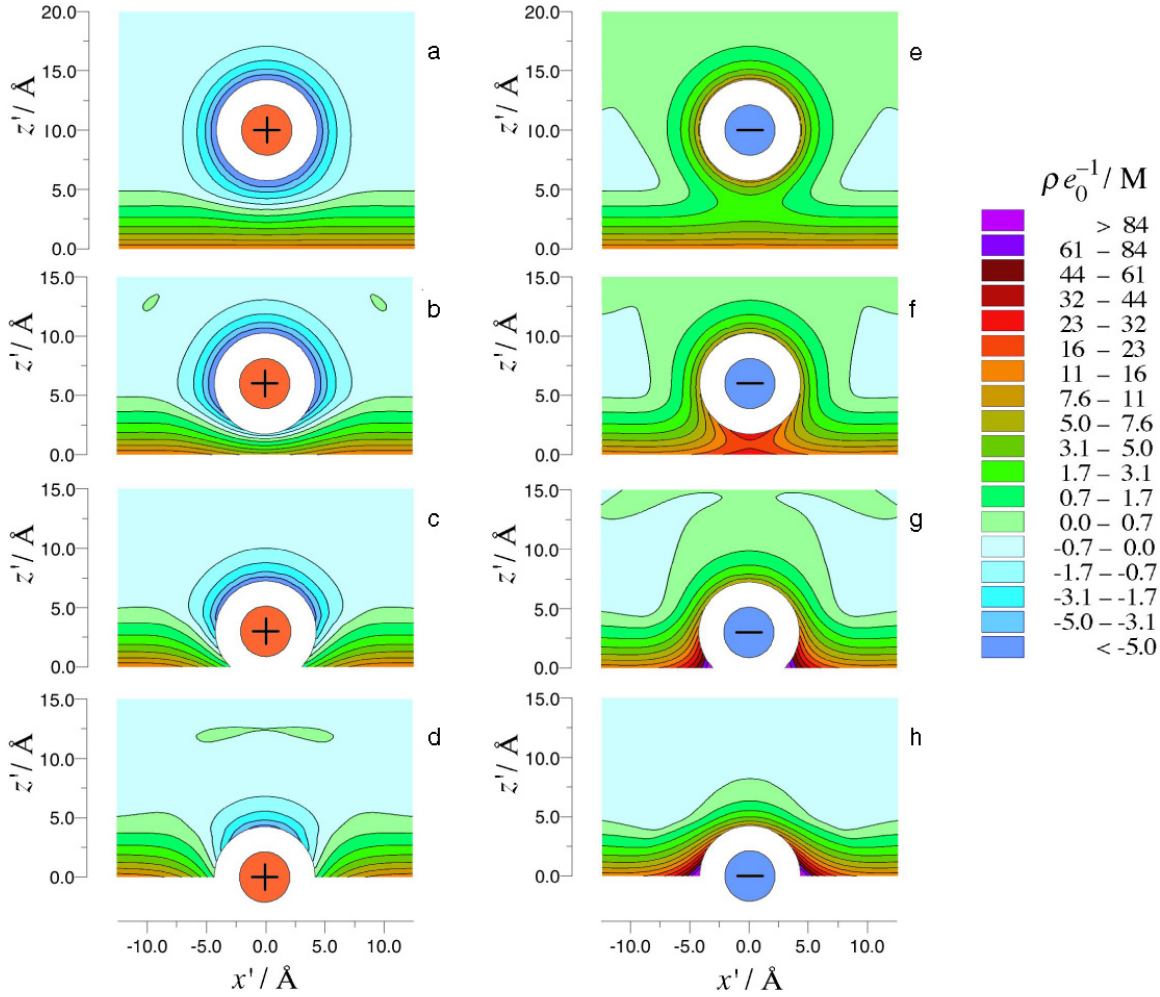

Figure 5. (a)–(d) Same charge density $\rho^{(2)}(\mathbf{r}'|z, i)$ as in figure 4(c) but for various positions, z, of a counterion (cation, $i = +$). In (a) $z = 10$, (b) $z = 6$, (c) $z = 3$ and (d) $z = 0$ Å (in the latter the ion is in contact with the wall surface, which lies below the figure). Panel (c) is the same as in figure 4(c). Panels (e)–(h) show the corresponding data for a coion (anion, $i = -$). In (e) $z = 10$, (f) $z = 6$, (g) $z = 3$ and (h) $z = 0$ Å. The density has cylindrical symmetry around a vertical axis through the centre of the ion in each case. (Figure based on data from [9].) Comment for greyscale printouts of the figure: the charge density is positive close to the wall in all panels. It is also positive around the anion in panels (e)–(h), while it is negative around the cation in panels (a)–(b) and around the upper half of the cation in panels (c)–(d).

distribution around ion I depends on the location of the ion, while the force from the surface charge is constant irrespective of distance (a standard result for the force from an planar sheet of charge with, in principle, infinite lateral extent).

In addition to the electrostatic force there is a force from the core–core interactions, i.e. from collisions on ion I from other ions that on average push the ion towards or away from the surface. We call this force $f_i^{\text{core}}(z)$. The total force

$$f_i(z) = f_i^{\text{el}}(z) + f_i^{\text{core}}(z) \tag{6}$$

is related to the potential of mean force $w_i(z)$ for the ion by

$$f_i(z) = -\frac{\mathrm{d}w_i(z)}{\mathrm{d}z} \tag{7}$$

and the density distribution is given by

$$n_i(z) = n_i^{\text{bulk}} \mathrm{e}^{-\beta w_i(z)}. \tag{8}$$

Thus an analysis of the forces gives the information needed to understand the behaviour of the density profiles and thereby phenomena like charge inversion. Consider the charge distribution around an ion of species i located at distance z from the surface, i.e. a distribution like that depicted in figure 5. We place the origin of the coordinate system at the line that goes through the ion centre and is perpendicular to the surface. The ion thereby has coordinates $\mathbf{r} = (0, 0, z)$. The charge distribution at point $\mathbf{r}' = (x', y', z')$ around the i ion located at z is denoted as $\rho^{(2)}(\mathbf{r}'|z, i)$, where the superscript (2) indicates that it is a pair distribution, i.e. a density around an ion (see the appendix, equation (18), for the formal definition). From Coulomb's law it follows that

$$f_i^{\text{el}}(z) = q_i \left[\frac{\sigma}{2\epsilon_{\text{r}}\epsilon_0} - \int \frac{z' - z}{4\pi\epsilon_{\text{r}}\epsilon_0 D^3} \rho^{(2)}(\mathbf{r}'|z, i)\, \mathrm{d}\mathbf{r}' \right], \tag{9}$$

where $D = [x'^2 + y'^2 + (z' - z)^2]^{1/2}$ is the distance from the ion centre to point $\mathbf{r}'$ and the integration is over all space. The first term in the square brackets is the force from σ on a unit charge and in the integral the factor $(z' - z)/D$ projects out the z component of the force while the remaining D^2 in the denominator comes from Coulomb's law.

The core–core collision force $f_i^{\text{core}}(z)$ acts on the surface of the ion when other ions collide with it (momentum transfer). The force from each collision is perpendicular to the surface of the ion and on average the pressure from all collisions at a particular point at the surface is proportional to the average contact density of ions there (it is the surface of the cavity around the ion, the sphere of radius a, that is considered here rather than the surface of the ion itself). The proportionality constant is $k_{\text{B}}T$, the same as for collision from an ideal gas (this is a consequence of the fact that the Maxwell–Boltzmann distribution of particle velocities holds in classical statistical mechanics, irrespective of the interactions). The contact density at the sphere surface can be calculated from the ion–ion pair distribution functions that we have available. From the cylindrical symmetry around the ion it follows that the density is the same for all points on the surface with the same coordinate z'. We denote the contact density at z' as $n^{\text{contact}}(z'|z,i)$, where z is the coordinate of the ion centre, as before (the formal definition of n^{contact} is given in the appendix, equation (19)). Note that n^{contact} is the total density for *all* species of ions present. The average core–core collision force on the ion equals

$$f_i^{\text{core}}(z) = -k_{\text{B}}T \int_{z-a}^{z+a} \frac{z'-z}{a}\, n^{\text{contact}}(z'|z,i) 2\pi a \,\mathrm{d}z', \quad (10)$$

where the factor $(z'-z)/a$ projects out the z component of the force and $2\pi a\,\mathrm{d}z'$ gives the area element on the sphere surface (the two a actually cancel in the integrand). The integrand is zero when $z' < 0$ since the density is zero there. For an ion in contact with the wall surface, $z = 0$, the integral is always positive because the only contribution comes from $z' > 0$ where the integrand is positive and hence $f_i^{\text{core}}(0) < 0$. This expresses the fact that an ion at $z = 0$ has collisions only on the outer half-sphere (on the solution side), which pushes it in the negative z direction (towards the surface).

In the analysis of the forces we will divide both f_i^{el} and f_i^{core} into two parts, the 'cavity' and 'polarization' contributions. The former is from the unperturbed density in the presence of the cavity of radius a around the ion. The latter is due to the polarization of the electrolyte outside the cavity from the electrostatic interactions with the ion and the core–core interactions. For f_i^{el} we therefore first consider a charge distribution like that depicted in figure 4(b), where the charge density outside the cavity is unperturbed. The electrostatic force that acts on the ion from the charge distribution $\rho(z)$ outside the cavity and zero inside is denoted $f_i^{\text{el(Cav)}}$, where 'Cav' stands for cavity. We also include the force from the surface charge density σ in $f_i^{\text{el(Cav)}}$ (this is necessary to obtain a finite force). The remainder of f_i^{el} is due to the fact that the charge density outside the ion in reality looks like that in figure 4(c), where the polarization is taken into account and we define

$$f_i^{\text{el(Pol)}}(z) = f_i^{\text{el}}(z) - f_i^{\text{el(Cav)}}(z), \quad (11)$$

where 'Pol' stands for polarization. The polarization part also contains the redistribution of charge needed to maintain local electroneutrality, $q_i + \int \rho^{(2)}(\mathbf{r}'|z,i)\,\mathrm{d}\mathbf{r}' = 0$.

The force $f_i^{\text{el(Cav)}}$, satisfies the following simple relationship [10]:

$$\frac{\mathrm{d}f_i^{\text{el(Cav)}}(z)}{\mathrm{d}z} = \frac{q_i}{2\epsilon_{\text{r}}\epsilon_0 a}\int_{z-a}^{z+a} \rho(z')\,\mathrm{d}z'. \quad (12)$$

For ions close to the surface a large part of the integration interval lies in $z' < 0$ where $\rho(z') = 0$. From equation (12) we obtain $f_i^{\text{el(Cav)}}(z)$ by integration from ∞ to z, where we put $f_i^{\text{el(Cav)}}$ to zero at infinity.

For f_i^{core} we can do the corresponding subdivision. When the unperturbed density is used outside the cavity, the contact density at z' is simply $\sum_j n_j(z')$, which should replace n^{contact} in equation (10). Then the force from the collisions becomes the same for an anion and a cation. Here we shall do something slightly better. The collisions on a cation will be dominated by anions since cations are repelled by the electrostatic interaction and will reach the surface to a lesser extent. The corresponding is true for collision on an anion. Therefore we take

$$\begin{aligned} f_+^{\text{core(Cav)}}(z) &= 2\pi k_{\text{B}}T \int_{z-a}^{z+a} (z-z')\, n_-(z')\,\mathrm{d}z' \\ f_-^{\text{core(Cav)}}(z) &= 2\pi k_{\text{B}}T \int_{z-a}^{z+a} (z-z')\, n_+(z')\,\mathrm{d}z' \end{aligned} \quad (13)$$

and define

$$f_i^{\text{core(Pol)}}(z) = f_i^{\text{core}}(z) - f_i^{\text{core(Cav)}}(z). \quad (14)$$

We expect that $f_i^{\text{core(Pol)}}$ is also dominated by collisions with ions of the opposite sign since they are attracted electrostatically to the surface of the ion, which makes the contact density large.

The total force on an ion in the case of unperturbed density profiles in the presence of the cavity is

$$f_i^{(\text{Cav})}(z) = f_i^{\text{el(Cav)}}(z) + f_i^{\text{core(Cav)}}(z)$$

and the total force from the polarization is

$$f_i^{(\text{Pol})}(z) = f_i^{\text{el(Pol)}}(z) + f_i^{\text{core(Pol)}}(z).$$

We shall compare $f_i^{(\text{Cav})}$ and $f_i^{(\text{Pol})}$ with the total force $f_i = f_i^{(\text{Cav})} + f_i^{(\text{Pol})}$ for the various cases in order to deduce how large an influence each of them has. We shall denote the component $f_i^{(\text{Cav})}$ as the 'cavity force' and $f_i^{(\text{Pol})}$ as the 'polarization force'.

6. Analysis of the forces; charge inversion mechanism

In figure 6 the various forces as functions of z are shown for the same 2:2 electrolyte system as discussed earlier. For easy reference, the ion density profiles $n_i(z)$ are also shown in the figure together with the corresponding PB prediction. The charge density profile for this system is shown in figures 1 and 4. Let us start with the force on a counterion, figure 6(b). For small z the total force $f_+(z)$ is strongly attractive (i.e. directed towards the surface), which according to equations (7)–(8) corresponds to the steeply increasing

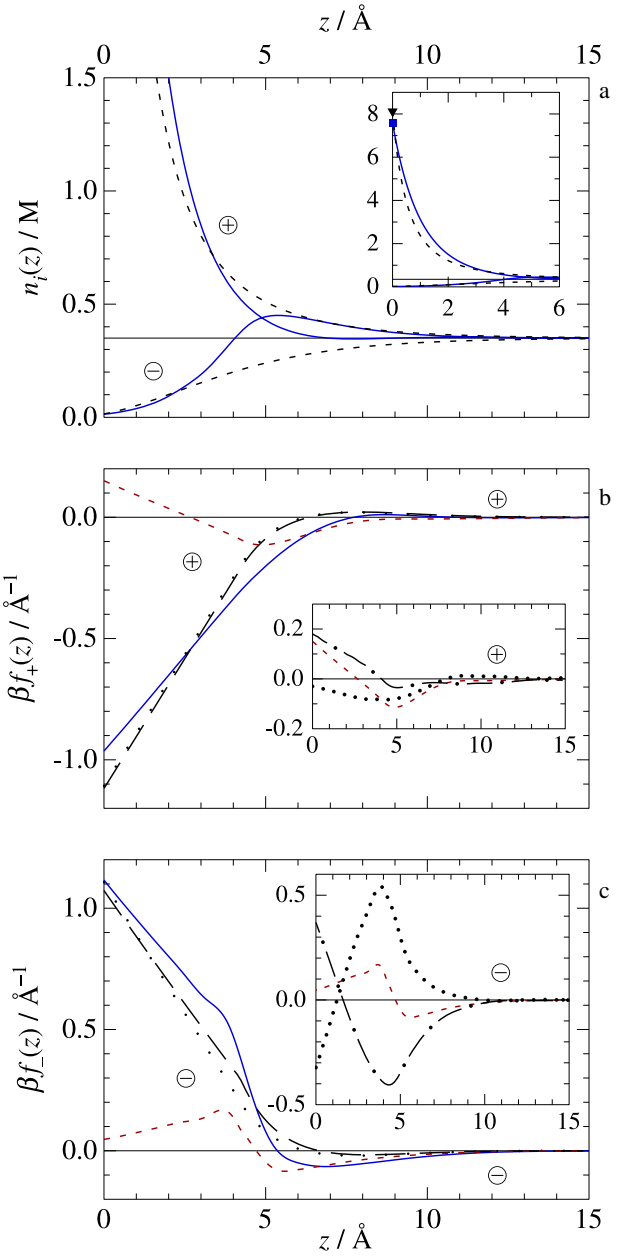

Figure 6. (a) The ion density profiles $n_i(z)$ for the same 2:2 electrolyte system as in figures 1, 4 and 5. The full lines show the profiles calculated with proper consideration of ion–ion correlations, while the dashed lines show the Poisson–Boltzmann (PB) prediction (marked ⊕ for cations and ⊖ for anions). The inset in (a) shows the same curves on a different scale. The counterion contact density is shown as a symbol: a filled square for the actual density and a filled triangle for the PB prediction. Panel (b) shows the forces on a counterion (cation) and panel (c) the forces on a coion (anion) as functions of the distance, z, from the charged surface in the same system. The full line shows the total force $f_i(z)$, the long dashes show the cavity force $f_i^{(\mathrm{Cav})}(z)$, the short dashes show the polarization force $f_i^{(\mathrm{Pol})}(z)$ and the sparse dots show the electrostatic part of the cavity force $f_i^{\mathrm{el(Cav)}}(z)$ (in panel (b) the latter virtually coincide with the $f_i^{(\mathrm{Cav})}$ curve). The insets of panels (b) and (c) show the polarization force (same as in the main plot) and its components: the dashed–dotted line shows the electrostatic part $f_i^{\mathrm{el(Pol)}}(z)$ and the dots show the contribution from core–core collisions $f_i^{\mathrm{core(Pol)}}(z)$. A force is positive when it is directed away from the surface (repulsion) and negative when it is directed towards the surface (attraction). (Based in part on data from [9].)

counterion density near the surface. By comparing $f_+^{(\mathrm{Cav})}$ and $f_+^{(\mathrm{Pol})}$ with the total f_+ in the figure we see that the cavity force constitutes by far the largest part of f_+ for $z < 3$ Å. In fact, the polarization force is *repulsive* for most of the z values where $n_+(z)$ exceeds the PB prediction. In 2.7 Å $< z <$ 6.4 Å both components contribute to the build up of counterion density there. Above $z = 8$ Å the contributions from $f_+^{(\mathrm{Cav})}$ and $f_+^{(\mathrm{Pol})}$ have similar magnitudes and are rather small.

For coions, figure 6(c), the situation is similar for small z (except for the sign). The total force f_- is strongly repulsive, which corresponds to the decreasing coion density near the surface, and it is dominated by $f_-^{(\mathrm{Cav})}$. In this case $f_-^{(\mathrm{Pol})}$ acts in the same direction for $z < 4.7$ Å. The attractive regime of f_- for $z > 5.4$ Å corresponds to the build up of the coion density peak around $z = 5.4$ Å in panel (a) of the figure. Here the polarization force gives the largest contribution, but the cavity force contributes somewhat to the attraction in an interval above $z > 6.7$ Å. As we shall see it is the electrostatic contribution to $f_-^{(\mathrm{Pol})}$ that gives the attraction, which hence causes the coion density peak.

Thus we can conclude that $f_i^{(\mathrm{Cav})}$ is the main component of the force that leads to the excess counterions near the surface. To see whether it is the electrostatic or the core collision contribution to $f_i^{(\mathrm{Cav})}$ that is most important, we have plotted the electrostatic one, $f_i^{\mathrm{el(Cav)}}$, in the figure. For counterions, the electrostatic contribution virtually coincides with $f_+^{(\mathrm{Cav})}$, so the core contribution is negligible. For coions, the core contribution is larger and gives rise to the difference between $f_-^{(\mathrm{Cav})}$ and $f_-^{\mathrm{el(Cav)}}$ seen in the figure. This is a consequence of appreciable contact densities from the large amount of counterions close to the wall surface. Overall, the electrostatic contribution is the most important part of $f_i^{(\mathrm{Cav})}$ for both coions and counterions.

Incidentally one should note that the electrostatic force from the unperturbed charge distribution in the *absence* of the cavity (i.e. calculated as in the PB approximation but based on the actual $\rho(z)$ in figure 1 rather than the PB profile) gives far too weak an attraction of counterions and repulsion of coions (not shown). Thus the presence of the cavity is essential here.

The main reason for the charge inversion can hence be described as follows. For a counterion in the vicinity of the surface, the hard core exclusion prevents other counterions to enter into the region between the ion and the surface. This effect is, for example, seen in figure 5(c) where the cavity makes the region between the ion and the surface void of ions. Thereby the surface charge becomes exposed (more exposed than if the cavity were absent) and can strongly attract the counterion. As noted above, the polarization around a counterion contributes to the attraction toward the surface when the counterion is located at $z > 2.7$ Å. This attraction is mainly caused by ion collisions on the outward (solution) side of the counterion, as will be further discussed below. In the PB approximation all these effects are absent and the counterions are free to enter the cavity, which reduces the attraction towards the surface charge.

The PB approximation also underestimates the repulsion of coions for similar reasons. For a coion close to the surface, the hard core exclusion effect makes the exposed surface

charge to strongly repel the ion, more strongly than in the PB approximation where counterions can enter into the cavity. As we have seen, polarization also contributes to the repulsion of the coion near the surface, which will be further discussed below.

Thus the electrostatic effects of the cavity constitute the main ingredient in the mechanism for charge inversion, but the polarization effects are also essential as they contribute to the build up of ionic density a few ångströms away from the surface. The reason why the polarization gives a relatively small contribution, $f_i^{(\mathrm{Pol})}$, to the total force can be found in the insets of figures 6(b) and (c), where its contributions $f_i^{\mathrm{el(Pol)}}$ and $f_i^{\mathrm{core(Pol)}}$ are plotted together with $f_i^{(\mathrm{Pol})}$ (which is $f_i^{\mathrm{el(Pol)}} + f_i^{\mathrm{core(Pol)}}$). For a coion the electrostatic and core contributions are quite large (panel (c)), but they cancel each other to a large extent. This can be explained as follows. When ions around the coion act with an attractive electrostatic force on the ion, they are themselves attracted to the ion and collide more frequently with it, i.e. the contact density becomes high. This leads to an increased repulsion that counteracts the electrostatic attraction (and vice versa for ions that are repelled electrostatically). In figures 5(f)–(h) we can see the reason for the large values of the electrostatic and core contributions to $f_-^{(\mathrm{Pol})}$. The counterions are strongly attracted to the region near the anion and the surface. In panels (f) and (g) this leads to a collisional repulsion of the anion away from the surface and an electrostatic attraction towards the surface. In panel (h) the counterion density is built up on the upper side of the anion (no ions can be on the other side), which leads to a collisional force towards the surface and an electrostatic force away from it, cf the inset of figures 6(c).

The enhancement of the collisional force from the interactions with the ion is illustrated in figure 7, where we compare $f_i^{\mathrm{core(Cav)}}$ with the total f_i^{core} plotted on different scales. Qualitatively the curves are remarkably similar, but f_i^{core} is about six times larger than $f_i^{\mathrm{core(Cav)}}$ for this system. The difference is due to the polarization effect; remember that $f_i^{\mathrm{core(Cav)}}$ is calculated solely from the unperturbed ion density profile of the oppositely charged species, equation (13).

For a counterion we see from figures 5(b)–(d) that the polarization is smaller than for a coion (anion) and in the inset to figure 6(b) we see that the electrostatic and core contributions to $f_+^{(\mathrm{Pol})}$ indeed are smaller compared to the inset to panel (c). The cancellation of the two contributions is less pronounced for a counterion, but it still exists for some z. An exception is the attraction around $z = 5$ Å, which is caused by both contributions; the collisional part is largest as mentioned above.

An important feature of figure 6(b) is that $f_+^{(\mathrm{Pol})}$ is repulsive near the surface, which is caused by the electrostatic part. As seen in the inset, the repulsion is only weakly counteracted by the collisional contribution for small z. In figure 5(d) we see that the reason for the electrostatic force in the direction away from the surface is that there is a negative charge density above the cation. This is caused by a rather high concentration of anions there (the remainder of the negative ion atmosphere of the counterion shown in figure 5(a)). These ions pull the cation away from the surface electrostatically and

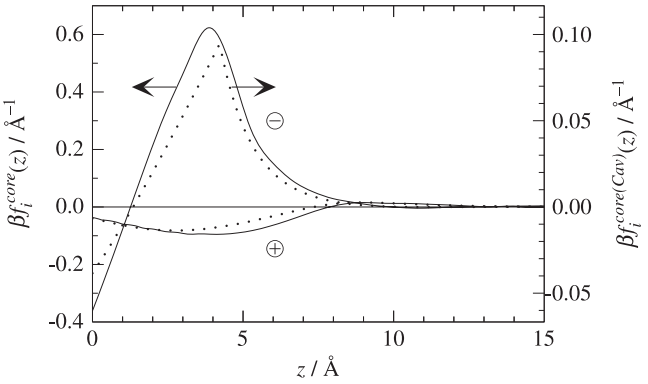

Figure 7. A comparison of the core–core collisional part $f_i^{\mathrm{core}}(z)$ of the total force (full curve) and the corresponding part $f_i^{\mathrm{core(Cav)}}(z)$ of the cavity force (dotted curve) on an cation and an anion (curves marked ⊕ and ⊖, respectively) for the same 2:2 electrolyte system as in figure 6. The ordinate scale to the left applies to the full curves and that to the right to the dotted curves.

hence they reduce the attraction towards the surface from the surface charge. In fact, this is the reason why the density of counterions at contact with the surface is lower than in the PB prediction, as can be seen in the inset of figure 6(a). Note that the total ionic concentration at contact is related to the bulk pressure, P^{bulk}, of the electrolyte solution via the contact theorem, which says that

$$k_{\mathrm{B}}T\sum_j n_j(0) - \frac{\sigma^2}{2\epsilon_{\mathrm{r}}\epsilon_0} = P^{\mathrm{bulk}} = k_{\mathrm{B}}T\sum_j n_j^{\mathrm{bulk}} + P^{\mathrm{bulk,ex}} \tag{15}$$

where $P^{\mathrm{bulk,ex}}$ is the excess pressure, i.e. the contribution to the pressure from ion–ion interactions in the bulk. In the PB approximation for electric double layers, which treats the bulk electrolyte like an ideal gas, we have $P^{\mathrm{bulk,ex}} = 0$, but otherwise equation (15) holds in this approximation. A lowering of the contact density of ions at the surface compared to the PB prediction is therefore equivalent to $P^{\mathrm{bulk,ex}} < 0$, i.e. that the ion–ion interactions act cohesively in the electrolyte solution. These facts emphasize the point that the charge inversion from ion–ion correlations is due to events that occur in the entire diffuse layer near the surface and not in some layer of ions in contact with the surface.

Applied to the case of an uncharged surface, equation (15) implies that $k_{\mathrm{B}}T\sum_j[n_j(0) - n_j^{\mathrm{bulk}}] = P^{\mathrm{bulk,ex}}$. The lowering of the total ion density near the surface seen in figure 3 for the 3:1 electrolyte is therefore congruent with $P^{\mathrm{bulk,ex}} < 0$. The force that pulls ions away from the uncharged surface originates from the ion atmosphere of each ion. This atmosphere has a total charge equal to the ionic charge but of opposite sign. For an ion in contact with the surface the atmosphere is entirely located on the side away from the surface—no ions can be located on the other side. Therefore the force is directed away from the surface. The charge of the atmosphere for a trivalent ion is larger than for a monovalent ion and hence the electrostatic force on the trivalent ion is larger. This is why the cation density in figure 3 is more affected near the surface than the anion density and is the cause of the charge separation

there. For a 2:2 electrolyte outside an uncharged surface the ionic density will decrease near the surface for the same reason. The anion and cation density will, however, be identical and there will be no charge separation in this case (provided the anions and cations only differ by the sign of their charges).

Let us now turn to a 3:1 electrolyte system with high surface charge density. In figure 8 the force curves are shown for the case 1.0 nm^2 per unit charge ($\sigma = -0.160$ C m^{-2}, same σ as for the 2:2 case in figure 6). The ion density profiles $n_i(z)$ are also shown in the figure together with the corresponding PB prediction. The charge density profile $\rho(z)$ for this system is the full line in figure 2. Qualitatively the results for the 3:1 system in figure 8 are similar to those for the 2:2 system in figure 6, but there are quantitative differences. For counterions, figure 8(b), we see that the cavity force dominates for small z in the region where the counterion density is larger than the PB prediction and we also see that the polarization force is attractive near the surface. This is like the 2:2 case. For $z \gtrsim 3$ Å the polarization contributes to a considerable extent to the build up of the counterion density, more so than in the 2:2 case. This is not surprising since the counterions have a larger valency here. The shallow concentration minimum for counterions around $z = 9$ Å is mainly caused by the repulsive cavity force in this region.

For coions, figure 8(c), we see that a repulsive cavity force dominates for small z, just as for the 2:2 case. It is the electrostatic part that gives the main contribution to this force. The coion density peak around $z = 5$ Å is caused by both the cavity and polarization forces which are attractive in a range above $z = 5$ Å. Compared to the 2:2 case, $f_-^{(\mathrm{Pol})}$ has a smaller influence, which is not surprising since the coions have a smaller valency here. Overall, it is $f_-^{(\mathrm{Cav})}$ that dominates nearly everywhere in the range shown.

It remains to consider the other 0.1 M 3:1 electrolyte systems of figure 2. Investigations of the forces for the systems with high surface charge densities, $\sigma = -0.267$ to about -0.064 C m^{-2} (corresponding to 0.6–2.5 nm^2 per unit charge) show essentially the same picture as in figure 8 and are not shown. The systems with low σ behave similarly to the uncharged case, see above.

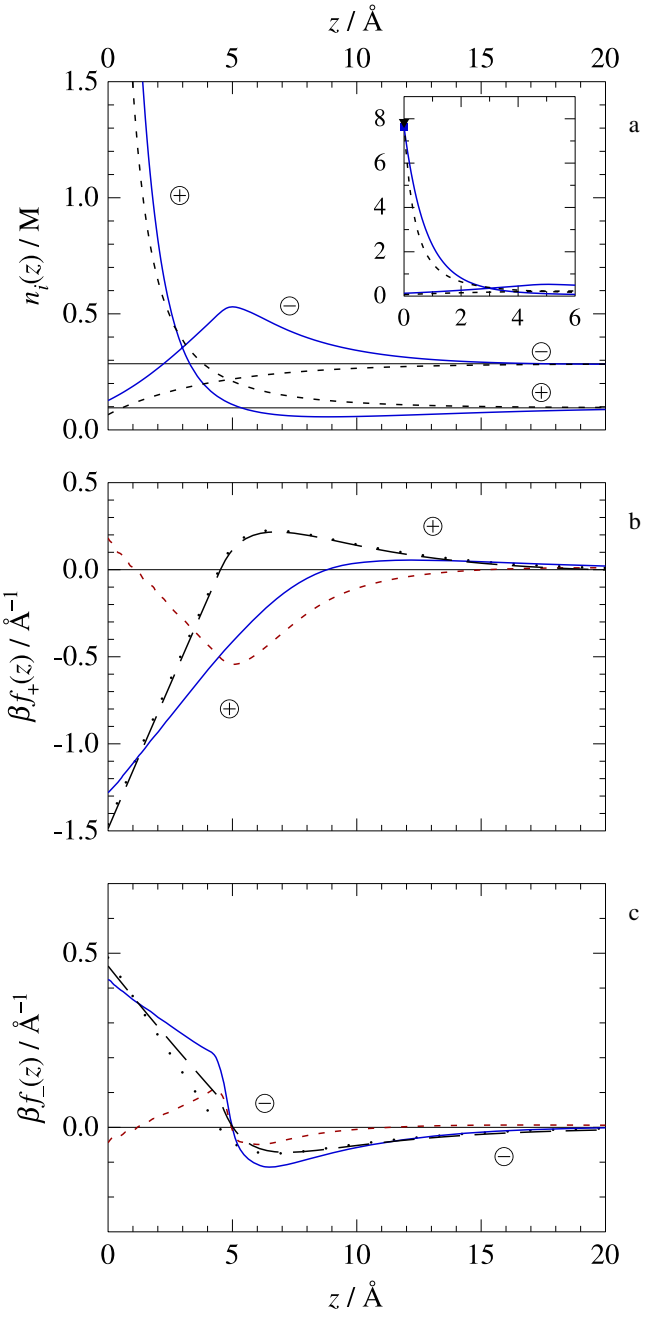

Figure 8. The same kind of curves as in figure 6 but for a 0.1 M 3:1 electrolyte system with surface charge density $\sigma = -0.160$ C m^{-2} (1.0 nm^2 per unit charge), i.e. the same system as for the full line in figure 2. The notation is the same as in figure 6.

7. Conclusions

To summarize we conclude that an analysis of the forces on the ions in the double layer gives detailed information about the mechanisms behind the structure of the double layer. The electrostatic effect from the excluded volume around each ion near the surface gives a very important contribution. The force on an ion from the charge density profile with a cavity around the ion (the electrostatic cavity force) dominates in the immediate vicinity of the surface, approximately the nearest few ångströms. There is also a force contribution from the polarization of the electrolyte surrounding an ion due to the interactions with the latter (the polarization force). Close to the surface this contribution is smaller than the cavity force, but it gives rise to a significant reduction in the contact density of ions at the surface. For an ion with low valency the cavity force gives a dominant contribution also a bit further away from the surface, while for ions with high valency the polarization effects give the dominant contribution there. The polarization force contains large contributions from both electrostatic interactions and ion–ion core collisions. These two contributions counteract each other to a large extent, so the net polarization force is appreciably smaller than each of them alone. The balance between these different effects is quite intricate in some regions.

As an example, the mechanism for charge inversion from ion–ion correlations was investigated and it was found that it is essentially the same for 2:2 and 1:3 electrolytes at high

surface charge densities σ. The electrostatic consequences of the excluded volume is, to a large extent, that the surface charge become exposed for ions close to the surface, so the unscreened surface charge can strongly attract counterions and repel coions. This contributes greatly to the effects that lead to charge inversion. If the presence of a cavity around each ion is neglected as in the Poisson–Boltzmann approximation, the ions that are then allowed to enter the exclusion zone will screen the surface charge to a large extent, which diminishes the net effect from the latter.

The polarization force is also essential for the charge inversion. It contributes to the build up of counterionic density a few ångströms away from the surface and a coion layer outside the counterion layer. This force is also neglected in the Poisson–Boltzmann approximation. The analysis of the mechanisms shows that events that take place in the entire diffuse layer are important for the understanding of charge inversion caused by ion–ion correlations. At least for conditions that are of relevance for aqueous electrolyte systems, it is not correct to think of the phenomenon as a property of some layer of ions in contact with the surface.

For the systems with lower σ the behaviour gradually approaches that of the uncharged surface when σ decreases, but the charge inversion remains for the 3:1 electrolyte, although to a small degree. For an uncharged surface there is a charge separation in the electrolyte and the surface behaves in many respects as if it has the same charge as the monovalent species. The consideration of the pair distributions for the ions near the surface gives insight into this behaviour. For symmetric 2:2 electrolytes the charge inversion eventually disappears when σ decreases towards zero and, furthermore, charge separation does not occur outside an uncharged inert surface for such electrolytes.

Appendix. Some aspects of the theory of distribution functions in inhomogeneous fluids

A.1. Integral equations

For an inhomogeneous fluid the particle density $n_i(z)$ and the pair distribution function $g_{ij}^{(2)}(\mathbf{r}_1, \mathbf{r}_2)$ satisfy the following *exact* relationships:

$$g_{ij}^{(2)}(\mathbf{r}_1, \mathbf{r}_2) = \mathrm{e}^{-\beta u_{ij}(\mathbf{r}_1,\mathbf{r}_2)+h_{ij}^{(2)}(\mathbf{r}_1,\mathbf{r}_2)-c_{ij}^{(2)}(\mathbf{r}_1,\mathbf{r}_2)+b_{ij}^{(2)}(\mathbf{r}_1,\mathbf{r}_2)} \tag{16}$$

and the Ornstein–Zernike equation

$$h_{ij}^{(2)}(\mathbf{r}_1, \mathbf{r}_2) = c_{ij}^{(2)}(\mathbf{r}_1, \mathbf{r}_2) + \sum_l \int h_{il}^{(2)}(\mathbf{r}_1, \mathbf{r}_3) n_l(z_3) c_{lj}^{(2)}(\mathbf{r}_3, \mathbf{r}_2)\, \mathrm{d}\mathbf{r}_3, \tag{17}$$

where u_{ij} is the pair interaction potential, $c_{ij}^{(2)}$ is the direct pair correlation function, $b_{ij}^{(2)}$ is the pair bridge function and $h_{ij}^{(2)} = g_{ij}^{(2)} - 1$. These equations are complemented by an additional *exact* equation for density distribution $n_i(z)$ in terms of the pair distribution functions. There are several alternatives [33] so none will be given explicitly here (see also [27–29]). The total set of equations can be solved provided the bridge function $b_{ij}^{(2)}$ can be expressed in terms of the other functions or is known by other means. In principle, $b_{ij}^{(2)}$ can be expressed *exactly* as a functional of all $h_{ij}^{(2)}$ and n_i, but in practice one must do some approximation for it (a closure approximation).

In the AHNC approximation [28] one sets $b_{ij}^{(2)} = 0$ and in the ARHNC approximation [27, 29] one takes $b_{ij}^{(2)}$ from a reference system; in our case an inhomogeneous hard-sphere mixture with the same density profiles as the inhomogeneous electrolyte. The pair distribution functions of the inhomogeneous hard-sphere system are analogously obtained by applying the Percus–Yevick closure, which gives very good results for such systems. The bridge function is then extracted and inserted in the equations for the electrolyte, which are then solved for $n_i(z)$ and $g_{ij}^{(2)}(\mathbf{r}_1, \mathbf{r}_2)$. Complete self-consistency is always attained for all functions involved in the numerical treatment. This is achieved by an iterational procedure.

For reference, we briefly describe the most common kind of integral equation approximations used for inhomogeneous fluids, where the only goal is to obtain the particle density $n_i(z)$. These approximations, which are *not* used in this work, are simpler and much less accurate. As an example we take the HNC/MSA approach, where one applies the HNC approximation for the one-particle distribution function $g_i(z) = n_i(z)/n_i^{\mathrm{bulk}}$. This function can be written analogously to equation (16) but for one-particle distribution functions and one sets the one-particle bridge function $b_i(z)$ to zero. To calculate the rest of the exponent, one utilizes the direct pair correlation function from the mean spherical approximation (MSA) for the *homogeneous* bulk fluid mixture with density n_i^{bulk} for each species.

A.2. Definitions of $\rho^{(2)}$ and $n^{contact}$

Here we give the formal definitions of $\rho^{(2)}(\mathbf{r}'|z, i)$ and $n^{\mathrm{contact}}(z'|z, i)$ in terms of the pair distribution functions. We assume that an ion is located at the point $\mathbf{r} = (0, 0, z)$, i.e. we have selected the origin of the coordinate system such that the x and y coordinates of the ion are zero. Then, we have

$$\rho^{(2)}(\mathbf{r}'|z, i) = \sum_j g_{ij}^{(2)}(\mathbf{r}, \mathbf{r}') n_j(z') q_j \tag{18}$$

and

$$n^{\mathrm{contact}}(z'|z, i) = \sum_j g_{ij}^{(2)}(\mathbf{r}, \mathbf{r}') n_j(z') \Big|_{\mathbf{r}' \text{ such that } |\mathbf{r}-\mathbf{r}'|=a} \quad \text{for } z - a \leqslant z' \leqslant z + a. \tag{19}$$

Note that the restriction on $\mathbf{r}'$ means that it lies on the surface of the sphere with radius a centred at $\mathbf{r}$ (i.e. the spherical cavity around the ion) and that the function is only defined in the range shown (otherwise $\mathbf{r}'$ cannot lie on the sphere surface). Due to the cylindrical symmetry around the ion, the value of $g_{ij}^{(2)}(\mathbf{r}, \mathbf{r}')$ only depends on z and z' when $|\mathbf{r} - \mathbf{r}'| = a$.

A.3. Interaction pressure between two planar walls

Let us consider the interaction pressure between two charged surfaces separated by distance H in the presence of an electrolyte as discussed in the Introduction of this paper. Here

H is the width of the slit available for the ionic centres. All ions are assumed to have diameter a. The pressure P in the slit between the surfaces (the perpendicular component of the pressure tensor) can be evaluated at the midplane of the slit, $z = H/2$. It consists of three parts, the ideal pressure $P^{\text{ideal}} = k_{\text{B}}T \sum_i n_i(H/2)$, the electrostatic correlation pressure, P^{el}, and the core–core collision pressure, P^{core}:

$$P(H) = P^{\text{ideal}}(H) + P^{\text{el}}(H) + P^{\text{core}}(H) \tag{20}$$

P^{el} arises because the ions on one side of the midplane correlate with the ions on the other side and give rise to an electrostatic pressure contribution between the surfaces. It is explicitly given by

$$P^{\text{el}}(H) = -\sum_{i,j} \int_{H/2}^{H} \mathrm{d}z\, n_i(z) \int_0^{H/2} \mathrm{d}z'\, n_j(z') \times \int \mathrm{d}\mathbf{R}\, \frac{\partial u_{ij}^{\text{Coul}}(|\mathbf{r}-\mathbf{r}'|)}{\partial z}\, h_{ij}(\mathbf{r},\mathbf{r}') \tag{21}$$

where the vector $\mathbf{R} = (x-x', y-y')$ lies in the lateral direction and $u_{ij}^{\text{Coul}}(r) = q_i q_j/(4\pi\epsilon_{\text{r}}\epsilon_0 r)$ is the Coulomb potential. P^{core} arises from collisions of ions on one side of the midplane with ions on the other side and it equals

$$P^{\text{core}}(H) = 2\pi\, k_{\text{B}}T \sum_{i,j} \int_{H/2}^{\min(H,a+H/2)} \mathrm{d}z\, n_i(z) \times \int_{\max(0,z-a)}^{H/2} \mathrm{d}z'\, n_j(z') \times (z-z') g_{ij}^{(2)}(\mathbf{r},\mathbf{r}')|_{\mathbf{r}' \text{ such that } |\mathbf{r}-\mathbf{r}'|=a}. \tag{22}$$

When the slit width H goes to zero $P^{\text{core}} \to 0$, which is due to the factor $z - z'$ in the integrand (both z and z' go to zero in this limit). The physical interpretation is that the ions can only collide in the lateral direction when $H = 0$, so there is no perpendicular pressure component from collisions. We shall now show that in the same limit $P^{\text{el}} \to -\sigma^2/(2\epsilon_{\text{r}}\epsilon_0)$, which is the main objective here.

By inserting u_{ij}^{Coul} and taking the z derivative in equation (21) we obtain

$$P^{\text{el}}(H) = \frac{1}{2\epsilon_{\text{r}}\epsilon_0} \sum_{i,j} \int_{H/2}^{H} \mathrm{d}z\, q_i n_i(z) \int_0^{H/2} \mathrm{d}z' q_j n_j(z') \times (z-z') \int_0^{\infty} \mathrm{d}R\, \frac{R\, h_{ij}(\mathbf{r},\mathbf{r}')}{[R^2+(z-z')^2]^{3/2}}. \tag{23}$$

where we have used $\mathrm{d}\mathbf{R} = 2\pi R\,\mathrm{d}R$ and $|\mathbf{r}-\mathbf{r}'| = [R^2 + (z-z')^2]^{1/2}$. We now split the R integral in two parts $\int_0^b$ and $\int_b^{\infty}$, where $0 < b < a$. The latter integral stays finite when $H \to 0$, which implies that the contribution from it in P^{el} goes to zero due to the factor $z - z'$. It remains to treat the contribution from the integral $\int_0^b$. We have $R < a$ so if H is sufficiently small we have $|\mathbf{r}-\mathbf{r}'| < a$ which implies that $h_{ij}(\mathbf{r},\mathbf{r}') = -1$ and hence we can do the R integral analytically. The result diverges like $-1/|z-z'|$ when $z - z' \to 0$ and hence the factor $z - z'$ in front of the integral in equation (23) is cancelled. Since electroneutrality implies that $\sum_i \int_{H/2}^{H} \mathrm{d}z\, q_i n_i(z) = \sum_j \int_0^{H/2} \mathrm{d}z' q_j n_j(z') = -\sigma$, we obtain the anticipated result

$$P^{\text{el}}(H) \to -\frac{\sigma^2}{2\epsilon_{\text{r}}\epsilon_0} \tag{24}$$

when $H \to 0$. The only limitation of this result for a slit with perfectly smooth surfaces (as in the model) is that one must be able to reach the limit $H \to 0$ before the counterions form a close-packed structure at the surface, which imposes an upper limit for σ for each ion diameter value a. (For atomic surfaces equation (24) is rather an approximate estimate.)

When $H \to 0$ the volume of the slit (per unit surface area) goes to zero like H. Only counterions will stay in the slit in this limit and there must remain $2|\sigma|/|q_{\text{counter}}|$ counterions per unit area, where q_{counter} is the counterion charge. Thus the ion concentration increases like $2|\sigma|/(H|q_{\text{counter}}|)$ so we have $P^{\text{ideal}}(H) = k_{\text{B}}T \sum_i n_i(H/2) \sim k_{\text{B}}T\, 2|\sigma|/(H|q_{\text{counter}}|)$. Thus

$$P(H) \sim k_{\text{B}}T \sum_i n_i(H/2) - \frac{\sigma^2}{2\epsilon_{\text{r}}\epsilon_0} \sim \frac{2k_{\text{B}}T\,|\sigma|}{H\,|q_{\text{counter}}|} \tag{25}$$

when $H \to 0$.

The pressure in the slit can alternatively be obtained from the contact theorem:

$$P(H) = k_{\text{B}}T \sum_j n_j(z=0;H) - \frac{\sigma^2}{2\epsilon_{\text{r}}\epsilon_0} \tag{26}$$

where the notation '; H' is used to explicitly show that the density profile is for a slit of width H (which we have suppressed in equations (21)–(25)). Incidentally, we note that the contact theorem in equation (15) is for the density $n_j(z = 0; \infty)$ in this notation and $P(\infty) = P^{\text{bulk}}$.

The pressure from equation (26) has the same value as that from equation (20) for all H provided the correct pair distributions and density profiles are used in the calculations. In particular, in the limit $H \to 0$ equation (26) gives the same behaviour for $P(H)$ as equation (25) since $\sum_j n_j(0) \sim \sum_j n_j(H/2)$ when the width vanishes. Equation (26) gives also a term $-\sigma^2/(2\epsilon_{\text{r}}\epsilon_0)$ in the pressure, but the origin of it is different compared to equation (24). (Note that the relationship between the contact density at a surface and the interactions in the electrolyte near the surface is not simple, see the discussion in section 6.)

The net pressure ΔP is the difference between the pressure in the slit and that in the bulk

$$\Delta P = P - P^{\text{bulk}}. \tag{27}$$

This is the relevant quantity for the interaction pressure between planar walls and it goes to zero when $H \to \infty$.

References

[1] Lyklema J 2006 *Colloids Surf.* A **291** 3
[2] Derjaguin B V and Landau L 1941 *Acta Phys. Chim. URSS* **14** 633

[3] Verwey E J W and Overbeek J Th G 1948 *Theory of the Stability of Lyophobic Colloids* (Amsterdam: Elsevier)
[4] Hill T L 1960 *An Introduction to Statistical Thermodynamics* (Reading, MA: Addison-Wesley) pp 359–61
[5] Oosawa F 1971 *Polyelectrolytes* (New York: Dekker) p 123
[6] Guldbrand L, Jönsson Bo, Wennerström H and Linse P 1984 *J. Chem. Phys.* **80** 2221
[7] Kjellander R and Marčelja S 1984 *Chem. Phys. Lett.* **112** 49
[8] Kjellander R, Åkesson T, Jönsson Bo and Marčelja S 1992 *J. Chem. Phys.* **97** 1424
[9] Kjellander R and Greberg H 1998 *J. Electroanal. Chem.* **450** 233
Kjellander R and Greberg H 1999 *J. Electroanal. Chem.* **462** 273 (erratum)
[10] Greberg H and Kjellander R 1998 *J. Chem. Phys.* **108** 2940
[11] Carnie S L and Torrie G M 1984 *Adv. Chem. Phys.* **56** 141
[12] Torrie G M, Valleau J P and Outhwaite C W 1984 *J. Chem. Phys.* **81** 6296
[13] Valleau J P and Torrie G M 1982 *J. Phys. Chem.* **86** 3251
[14] Lozada-Cassou M, Saavedra-Barrera R and Henderson D 1982 *J. Chem. Phys.* **77** 5150
[15] Outhwaite C W and Bhuyian L B 1983 *J. Chem. Soc. Faraday Trans.* II **79** 707
[16] Grosberg A Yu, Nguyen T T and Shklovskii B I 2002 *Rev. Mod. Phys.* **74** 329
[17] Quesada-Pérez M, González-Tovar E, Martín-Molina A, Lozada-Cassou M and Hidalgo-Álvarez R 2003 *ChemPhysChem* **4** 234
[18] Messina R 2009 *J. Phys.: Condens. Matter* **21** 113102
[19] Messina R, González-Tovar E, Lozada-Cassou M and Holm C 2002 *Europhys. Lett.* **60** 383
[20] Jiménez-Ángeles F and Lozada-Cassou M 2004 *J. Phys. Chem.* B **108** 7286
[21] Kjellander R and Mitchell D J 1992 *Chem. Phys. Lett.* **200** 76
Kjellander R and Mitchell D J 1994 *J. Chem. Phys.* **101** 603
[22] Attard P 1993 *Phys. Rev.* E **48** 3604
[23] Ennis J, Marčelja S and Kjellander R 1996 *Electrochim. Acta* **41** 2115
[24] Ulander J, Greberg H and Kjellander R 2001 *J. Chem. Phys.* **115** 7144
[25] Evans R, Leote de Carvalho R J F, Henderson J R and Hoyle D C 1994 *J. Chem. Phys.* **100** 591
[26] Torrie G M and Valleau J P 1980 *J. Chem. Phys.* **73** 5807
[27] Greberg H and Kjellander R 1994 *Mol. Phys.* **83** 789
[28] Kjellander R and Marčelja S 1985 *J. Chem. Phys.* **82** 2122
[29] Greberg H, Kjellander R and Åkesson T 1997 *Mol. Phys.* **92** 35
[30] Valleau J P, Ivkov R and Torrie G M 1991 *J. Chem. Phys.* **95** 520
[31] Belloni L 1993 *J. Chem. Phys.* **98** 8080
[32] Raineri F O and Stell G 2001 *Condens. Matter Phys.* **4** 621
[33] Rowlinson J S and Widom B 1989 *Molecular Theory of Capillarity* (Oxford: Clarendon)